Accepted Manuscript

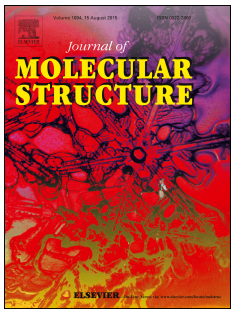

Crystal structures and DFT calculations of mixed chloride-azide zinc(II) and chloride-isocyanate cadmium(II) complexes with the condensation product of 2-quinolinecarboxaldehyde and Girard's T reagent

Katarina Anđelković, Andrej Pevec, Sonja Grubišić, Iztok Turel, Božidar Čobeljić, Milica R. Milenković, Tanja Keškić, Dušanka Radanović

PII: S0022-2860(18)30226-6

DOI: 10.1016/j.molstruc.2018.02.074

Reference: MOLSTR 24896

To appear in: *Journal of Molecular Structure*

Received Date: 16 January 2018

Revised Date: 19 February 2018

Accepted Date: 19 February 2018

Please cite this article as: K. Anđelković, A. Pevec, S. Grubišić, I. Turel, Bož. Čobeljić, M.R. Milenković, T. Keškić, Duš. Radanović, Crystal structures and DFT calculations of mixed chloride-azide zinc(II) and chloride-isocyanate cadmium(II) complexes with the condensation product of 2-quinolinecarboxaldehyde and Girard's T reagent, *Journal of Molecular Structure* (2018), doi: 10.1016/j.molstruc.2018.02.074.

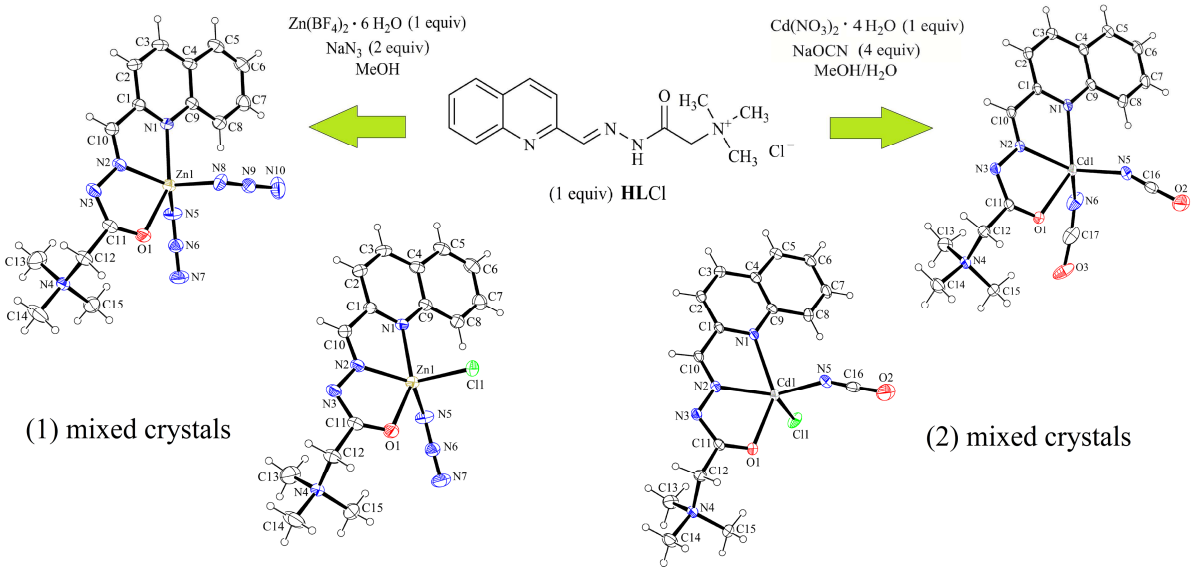

Crystal structures and DFT calculations of mixed chloride-azide zinc(II) and chloride-isocyanate cadmium(II) complexes with the condensation product of 2-quinolinecarboxaldehyde and Girard's T reagent

Katarina Anđelković,[a] Andrej Pevec,[b] Sonja Grubišić,[c] Iztok Turel,[b] Božidar Čobeljić,[a] Milica R. Milenković,[a] Tanja Keškić[a] and Dušanka Radanović,*[c]

[a]*Faculty of Chemistry, University of Belgrade, Studentski trg 12-16, 11000 Belgrade, Serbia*
[b]*Faculty of Chemistry and Chemical Technology, University of Ljubljana, Večna pot 113, 1000 Ljubljana, Slovenia*
[c]*Institute of Chemistry, Technology and Metallurgy, University of Belgrade, Njegoševa 12, P.O. Box 815, 11000 Belgrade, Serbia*

Abstract

The mixed chloride-azide $[Zn\mathbf{L}(N_3)_{1.65}Cl_{0.35}]$ (**1**) and chloride-isocyanate $[Cd\mathbf{L}(NCO)_{1.64}Cl_{0.36}]$ (**2**) complexes with the condensation product of 2-quinolinecarboxaldehyde and trimethylammonium acetohydrazide chloride (Girard's T reagent) (**HL**Cl) have been prepared and characterized by X-ray crystallography. In complexes **1** and **2**, Zn1 and Cd1 ions, respectively, are five-coordinated in a distorted square based pyramidal geometry with NNO set of donor atoms of deprotonated hydrazone ligand and two monodentate ligands N_3^- and/or N_3^- and Cl^- in the case of **1** and OCN^- and/or OCN^- and Cl^- in the case of **2**. The structural parameters of **1** and **2** have been discussed in relation to those of previously reported M(II) complexes with the same hydrazone ligand. Density functional theory calculations have been employed to study the interaction between the Zn^{2+} and Cd^{2+} ions and ligands. High affinity of ligands towards the Zn^{2+} and Cd^{2+} ions are predicted for both complexes.

Keywords: Zn(II) and Cd(II) complexes, hydrazones, mixed crystals, DFT

* Corresponding author: Dušanka Radanović, e-mail: radanovic@chem.bg.ac.rs

1. Introduction

Hydrazones are multipurpose class of ligands having notable biological and chemical activities [1–5]. Therefore, the design and preparation of new complexes with d-metals and hydrazone based ligands with aim to improve ~~and tune the~~ their proprieties through the discovery of new structures is still a great scientific challenge. A basic possibility to improve the structural features of the hydrazone based complexes is the use of auxiliary ligands, such as pseudohalides (N_3^-, NCS^-, NCO^-, etc.). These are versatile ligands which can be coordinated as monodentates [6–8] or as bridges between metal centers in the end-to-end or end-on bridging modes [9–11]. Homoatomic azido ligand exhibits many bridging coordination modes (Scheme 1): single and double $\mu_{1,3}$-N_3 (end-to-end, EE) and $\mu_{1,1}$-N_3 (end-on, EO), $\mu_{1,1,3}$-N_3, $\mu_{1,1,1}$-N_3, $\mu_{1,1,1,1}$-N_3, $\mu_{1,1,3,3}$-N_3, and $\mu_{1,1,1,3,3,3}$-N_3 [10]. Cyanate as an ambidentate ligand exhibits linkage isomerism and may be coordinated through nitrogen or oxygen donor atoms as monodentate or bridging ligand (end-on $\mu_{1,1}$-κ_N and $\mu_{1,1}$-κ_O or end-to-end $\mu_{1,3}$) [11]. Exchange interactions between two paramagnetic centers which propagate through discrete polyatomic bridging moieties (N_3^-, NCS^-, NCO^-, etc.) have been the subject of several reviews focusing on the ability of these pseudohalide ligands to coordinate with metals in a variety of ways [12–14].

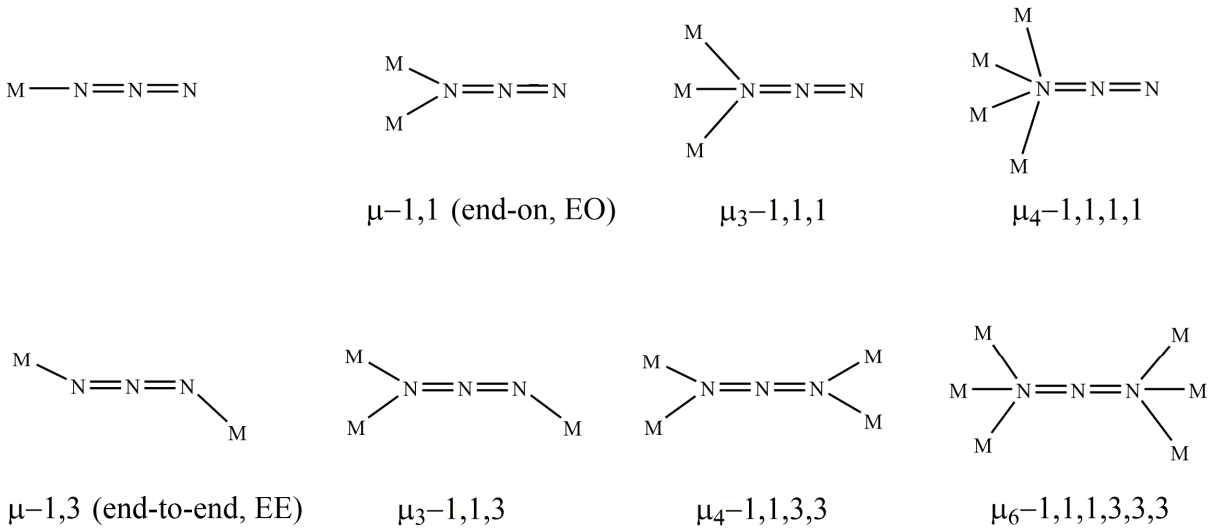

Scheme 1. Coordination modes of azido ligand.

Recently, we have reported the crystal structures of a series of d-metal complexes with the condensation product of 2-quinolinecarboxaldehyde and trimethylammonium acetohydrazide chloride (**HL**Cl, Scheme 2) and N_3^-, OCN^- or Cl^- as auxiliary ligands ([Co**HL**$(N_3)_3$] [15], [Co_2**L**$_2$(μ-$_{1,1}$-N_3)$_2$(N_3)$_2$]·H_2O·CH_3OH [15], [Ni_2**L**$_2$(μ-$_{1,1}$-N_3)$_2$(N_3)$_2$]·H_2O·CH_3OH [16], [Zn**L**$(N_3)_2$] [17], [Zn**L**$(NCO)_2$] [17] and [Cd**L**Cl_2]·CH_3OH [18]). The geometry and

nuclearity of these coordination complexes are directed by a central metal ion and ligand's charge. Nickel(II) ion with **HL**Cl and N_3^- preferred the formation of dinuclear ferromagnetically coupled di-($\mu_{1,1}$-azido) complex of octahedral geometry [16]. However, Co(II) ion with **HL**Cl and N_3^- preferred the formation of octahedral mononuclear [Co**HL**$(N_3)_3$] complex, while the dinuclear ferromagnetically coupled [Co_2**L**$_2$($\mu_{1,1}$-$N_3)_2(N_3)_2]\cdot H_2O\cdot CH_3OH$ [15] complex has been obtained in traces. Coordination of metal ions (Zn(II) and Cd(II)) with **HL**Cl and N_3^-, OCN^- or Cl^- as auxiliary ligands afforded the formation of mononuclear complexes of distorted square pyramidal geometry [17,18]. As a continuation of our study of d-metal complexes with the condensation product of 2-quinolinecarboxaldehyde and trimethylammonium acetohydrazide chloride (**HL**Cl), here, we report the crystal structures and DFT calculations of mixed chloride-azide [Zn**L**$(N_3)_{1.65}Cl_{0.35}$] (**1**) and chloride-isocyanate [Cd**L**$(NCO)_{1.64}Cl_{0.36}$] (**2**) complexes.

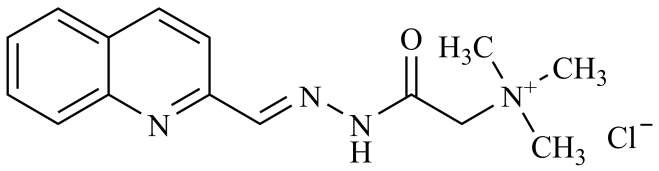

Scheme 2. Structure of (*E*)-*N*,*N*,*N*-trimethyl-2-oxo-2-(2-(quinolin-2-ylmethylene)hydrazinyl)ethan-1-aminium chloride (**HL**Cl)

2. Experimental section

2.1. Synthesis

*2.1.1. Synthesis of azidochloro(E)-N,N,N-trimethyl-2-oxo-2-(2-(quinolin-2-ylmethylene)hydrazinyl)ethan-1-aminium zinc(II) complex [Zn**L**$(N_3)_{1.65}Cl_{0.35}$] (**1**)*

In the previously reported reaction of **HL**Cl with $Zn(BF_4)_2\cdot 6H_2O$ and NaN_3 in the molar ratio 1 : 1 : 2 in methanol diazido Zn(II) complex [Zn**L**$(N_3)_2$] was obtained as a main product together with a trace of complex **1** [17]. Due to low quantity of complex **1** its structure is determined only in solid state by X-ray analysis.

*2.1.2. Synthesis of chloroisocyanato(E)-N,N,N-trimethyl-2-oxo-2-(2-(quinolin-2-ylmethylene)hydrazinyl)ethan-1-aminium cadmium(II) complex [CdL$(NCO)_{1.64}Cl_{0.36}$] (**2**)*

Few crystals of complex **2** were obtained in the previously reported reaction of **HL**Cl with $Cd(NO_3)_2 \cdot 4H_2O$ and NaOCN in molar ratio 1 : 1 : 4 in methanol/water mixture together with the main product [Cd**L**$(NCO)_2$] [18]. Since low amount of complex **2** was obtained its structure is determined only in solid state by X-ray analysis. Crystal structure of the main product of this reaction [Cd**L**$(NCO)_2$] was not determined due to inappropriate quality of obtained crystals. Its structure was proposed from the results of elemental analysis, NMR spectra, molar conductivity and DFT calculations, as it was previously described [18].

2.2. X-ray structure determinations

The molecular structure of complexes **1** and **2** were determined by single-crystal X-ray diffraction methods. Crystallographic data and refinement details are given in Table 1. The X-ray intensity data for **1** were collected at room temperature with Nonius Kappa CCD diffractometer with graphite-monochromated MoKα radiation (λ = 0.71073 Å) and processed using DENZO-SMN [19]. The X-ray intensity data for **2** were collected at 150 K with Agilent SuperNova dual source diffractometer using an Atlas detector and equipped with mirror-monochromated MoKα radiation (λ = 0.71073 Å). The data were processed using CRYSALIS PRO [20]. Both structures were solved by direct methods (SIR-92) [21] and refined by full-matrix least-squares procedures based on F^2 (SHELXL-2016) [22]. All non-hydrogen atoms were refined anisotropically. The C10 bonded hydrogen atoms in both structures were located in a difference map and refined with the distance restraints (DFIX) with C–H = 0.98 Å for **1** and C–H = 1.00 Å for **2** and with U_{iso}(H) = 1.2U_{eq}(C). All other hydrogen atoms were included in the model at geometrically calculated positions and refined using a riding model. Both structures are mixed crystals and were refined with the use of PART instructions [23]. The occupancy of N^{3-} and Cl^- in **1** was refined to a ratio of 64.7% and 35.3%, the ratio of OCN^- and Cl^- in **2** was found to be 63.6% and 36.4%. ORTEP-3 for Windows was used to prepare drawings [24].

2.3. Computational details

Density functional theory was used to determine the optimized geometries, and to calculate the interaction energies of Cd^{2+} and Zn^{2+} with ligands. All the DFT calculations were performed in gas phase with the Gaussian 09 [25] program at B3LYP level [26, 27]: the basis set used were LANL2DZ [28] for Cd and Zn atoms as well as 6-31G(d) [29] for the other

atoms. In addition, solvent effects for the free metal ions are calculated in water and methanol. Calculations were carried on the PARADOX supercomputing facility [30].

3. Results and discussion

*3.1. Crystal structures of **1** and **2***

Mixed chloride-azide [Zn**L**$(N_3)_{1.65}Cl_{0.35}$] (**1**) and chloride-isocyanate [Cd**L**$(NCO)_{1.64}Cl_{0.36}$] (**2**) complexes have been obtained in the reactions of (*E*)-*N*,*N*,*N*-trimethyl-2-oxo-2-(2-(quinolin-2-ylmethylene)hydrazinyl)ethan-1-aminium chloride (**HL**Cl) and the corresponding Zn^{2+} and Cd^{2+} salts by adding the NaN_3 and NaOCN, respectively. The molecular structures of **1** and **2** are displayed in Figs. 1 and 2, respectively. Selected bond lengths and angles of **1** and **2** are given in Table 2. The solid state structure of **1** is a superimposed 65 : 35 mixture of di- and mono-azide complexes [Zn**L**$(N_3)_2$] and [Zn**L**(N_3)Cl]. The structure of complex **2** is a superimposed 64 : 36 mixture of di- and mono-isocyanate complexes [Cd**L**$(NCO)_2$] and [Cd**L**(NCO)Cl]. In complexes **1** and **2**, Zn1 and Cd1 ions, respectively, adopt fivefold coordination with tridentate ligand **L** and two monodentate ligands N_3^- and/or N_3^- and Cl^- in **1** and OCN^- and/or OCN^- and Cl^- in **2**. The ligand **L** is coordinated to metallic centers (Zn1 and Cd1) in the zwitter-ionic form through NNO set of donor atoms forming two fused five-membered chelation rings. The dihedral angles between two five-membered chelation rings fused along Zn1-N2 and Cd1-N2 bonds in **1** and **2** are 4.2° and 1.8°, respectively. Other complexes [Zn**L**$(N_3)_2$] [17], [Zn**L**$(NCO)_2$] [17] and [Cd**L**Cl_2]·CH_3OH [18] with the same ligand **L** show greater deviation from planarity of the metal-ligand system, as evidenced by larger values of 5.7°, 6.2° and 11.1°, respectively, of the corresponding dihedral angles. The distortion in the five coordinated systems is described by an index of trigonallity $\tau = (\beta - \alpha)/60$, where β is the greatest basal angle and α is the second greatest angle [31]. The parameter τ is 0 for regular square based pyramidal forms and 1 for trigonal bipyramidal forms. The τ value of 0.33 calculated for **1** (for both complex species [Zn**L**$(N_3)_2$] and [Zn**L**(N_3)Cl]), indicates that the irregular coordination geometry about Zn1 is 33% trigonally distorted square based pyramidal. The Zn1 is lifted out of the plane of the four in-plane ligand atoms (N1, N2, N5 and O1) by a distance ρ of 0.5648(2) Å. The coordination geometry about Cd1 in **2** is 18% trigonally distorted square based pyramidal. The Cd1 is lifted out of the plane of the four in-plane ligand atoms (N1, N2, N5 and O1) by a distance ρ of 0.7072(3) Å. The

Zn(II) complexes are more trigonally distorted from ideal square based pyramidal configuration compared with the Cd(II) complexes with the same chelate ligand (**L**), as indicated by calculated τ values of 0.04, 0.18, 0.31, 0.33, and 0.34 for [Cd**L**Cl_2]·CH_3OH [18], complex **2**, [Zn**L**$(N_3)_2$] [17], complex **1** and [Zn**L**$(NCO)_2$] [17], respectively. The metal-ligand bonds in complex **2** are longer than corresponding ones in complex **1** (Table 2), as expected for larger metal ion of d^{10} configuration. The Zn1-N5-N6 and Zn1-N8-N9 angles between Zn(II) and the N_3^- ligands are 118.8(2)° and 120.8(9)°, respectively, reflecting the bent coordination of the azido ligands. The azido ligands are quasi linear with the N5-N6-N7 and N8-N9-N10 angles being 176.7(2)° and 176.2(8)°, respectively. The N-N bond distances in disordered N_3^- group are almost equivalent (N8-N9 = 1.155(11) Å and N9-N10= 1.159(8) Å). The ordered N_3^- group exhibits relatively asymmetric N-N bond distances (N5-N6 = 1.185(3) Å and N6-N7=1.152(3) Å) which are comparable to those observed in [Co**HL**$(N_3)_3$] [15]. The shorter $N_{(azido)}$–$N_{(azido)}$ bonds are more remote from the metal atom. The geometric parameters of OCN^- anions in **2** are: Cd1-N5-C16 = 155.3(4)°, Cd1-N6-C17 = 119.5(8)°, N5-C16-O2 = 177.4(5) °, N6-C17-O3 = 173.9(10)°, N5-C16 = 1.078(5) Å, C16-O2 = 1.212(6) Å, N6-C17 = 1.30(2) Å, and C17-O3 = 1.371(11) Å. The N-C and C-O bond distances observed in ordered OCN^- group are similar to those observed in [Zn**L**$(NCO)_2$] [17] complex. The disordered OCN^- group exhibits significantly longer N-C and C-O bonds.

In the crystals of **1** complex molecules connected by intermolecular interactions of C-H···π(quinoline ring) type form chains running parallel with *c*-axis direction. The neighboring chains are linked *via* intermolecular π···π interactions between quinoline rings related through the center of symmetry at 000 (Fig. 3). The shortest distance is between the centers of gravity of the pyridine rings and sums 3.6481(12) Å. Geometric parameters describing C-H···π and π···π interactions are listed in Tables 3 and 4, respectively. Similar chain-like motif parallel with *a* axis was observed in the crystals of octahedral [Co**HL**$(N_3)_3$] complex [15]. In the crystals of [Co**HL**$(N_3)_3$] [15] the neighboring chains are also linked *via* intermolecular π···π interactions between quinoline rings. In the crystals of **2** complex molecules form dimer around the center of symmetry at 0 ½ ½ *via* intermolecular π···π contact between quinoline rings (Fig. 4). The shortest distance of 3.544(2) Å is observed between the centers of gravity of the pyridine rings (Table 4). In the crystals of **2** no interaction of C-H···π(quinoline ring) type was observed.

3.2. DFT optimized structures and calculated interaction energies

In order to calculate the ground-state geometries of the complexes **1** and **2**, DFT calculations of di- and mono-azide complexes [Zn**L**$(N_3)_2$] and [Zn**L**(N_3)Cl], as well as di- and mono-isocyanate complexes [Cd**L**$(NCO)_2$] and [Cd**L**(NCO)Cl] have been performed, as described above. DFT calculations predict fivefold coordination for both Zn(II) and Cd(II) complexes with tridentate ligand **L** and two monodentate ligands N_3^- and/or N_3^- and Cl^- in complex **1** and OCN^- and/or OCN^- and Cl^- in **2** (Fig. 5), thereby supporting the experimental XRD results. Selected bond lengths and values of valence angles are summarized in Table S1 in the supplementary material. The calculated geometric parameters of mixed ligand complexes are compared with the X-ray diffraction structures and show good agreement. The highest occupied and lowest unoccupied molecular orbitals (HOMO and LUMO) and their energies were calculated to locate the high and low density regions in both complexes and are shown in Fig.6. The HOMOs of all complexes are delocalized mainly at the linear monodentate ligands N_3^- and/or N_3^- and Cl^- in complex **1** and OCN^- and/or OCN^- and Cl^- in **2** and metal centers, whereas the LUMOs are delocalized on the planar ring of Schiff base in equatorial plane (Fig. 6). Influences of monodentate ligands N_3^-, Cl^- and OCN^- ligands in **1** and **2** are estimated by comparing energies of frontier molecular orbitals (E_{LUMO}, E_{HOMO}) and their energy gap (Egap). Substitution of N_3^- / OCN^- with Cl^- ligands in complexes **1** and **2** has the similar influence on HOMO and LUMO energy levels (Fig. 6). Since azido group is stronger electron donating group in comparison to isocyanato, the Zn(II) complexes have smaller energy gap in comparison to Cd(II) complexes. Similarly, stabilization of HOMO orbitals is larger for monoazido/monoisocyanato and mono chloro Zn(II) and Cd(II) complexes in comparison to di-azide Zn(II) and di-isocyanato Cd(II) complexes, respectively.

In order to explain the factors responsible for the formation of mixed chloride-azide Zn(II) (**1**) and chloride-isocyanate Cd(II) (**2**) complexes we calculated the intrinsic binding energies of metal ions, using the density functional theory by considering in vacuo conditions and then taking the solvent effect for the free metal ions in water and methanol into consideration. The binding energy between the ligands and each metal in vacuo or water is defined as: ΔE(binding energy) = E(metal-binding ligands in vacuo) − [E(ligands in vacuo) + E(free metal ion in vacuo or water)].

The solvation energy of each free metal ion was calculated using the DFT method with a metal ions coordinated by six water molecules in the octahedral geometry as a solvation model. Furthermore, PCM model [32-36] was used to calculate the solvation effect for the surrounding water and methanol molecules under conditions that are similar to the experimental ones. The calculated absolute metal-binding energies in vacuo are presented in

Table 6 (intrinsic binding energies). The binding energies which take in account the solvation effect for free metal ions are also shown in Table 6 (real metal-binding energies). The results of this part of the study allow us to suggest that corresponding ligands have high affinity towards the Zn(II) and Cd(II) ions under experimental conditions. Further, these results provided good explanation of the possibility of Zn(II) and Cd(II) to efficiently bind two monodentate ligands N_3^- and/or N_3^- and Cl^- in complex **1** and OCN^- and/or OCN^- and Cl^- in complex **2**.

Conclusion

Zn(II) and Cd(II) ions with the condensation product of 2-quinolinecarboxaldehyde and trimethylammonium acetohydrazide chloride (**HL**Cl) form five coordinate complexes [Zn**L**X_2] (X = N_3^- or OCN^-) [17], [Cd**L**X_2] (X = Cl^- or OCN^-) [18], **1** and **2** of distorted square-based pyramidal geometry. The Zn(II) complexes display the greater degree of trigonal distortion from the square-based pyramidal coordination geometry compared with the Cd(II) complexes. The crystalline [Zn**L**$(N_3)_{1.65}Cl_{0.35}$] (**1**) and [Cd**L**$(NCO)_{1.64}Cl_{0.36}$] (**2**) complexes were obtained from the reaction solutions containing the [Zn**L**$(N_3)_2$] [17] and [Cd**L**$(NCO)_2$] [18] complexes, respectively, as the main products of the corresponding chemical reactions. We calculated the binding energies of metals to all ligands in complexes **1** and **2** by DFT and by considering the solvent effects for free metal ions. These results give theoretical explanation of the possibility of Zn(II) and Cd(II) to efficiently bind two monodentate ligands N_3^- and/or N_3^- and Cl^- in complex **1** and with OCN^- and/or OCN^- and Cl^- in **2**.

Acknowledgement

This work was supported by the Ministry of Education, Science and Technological development of the Republic of Serbia (Grant OI 172055) and Slovenian Research Agency (P-0175). We thank the EN-FIST Centre of Excellence, Ljubljana, Slovenia, for use of the SuperNova diffractometer.

Supplementary data

Crystallographic data for structures have been deposited at the Cambridge Crystallographic Data Centre as supplementary publication CCDC 1816621 and 1816622 for **1** and **2**, respectively. These data can be obtained free of charge via www.ccdc.cam.ac.uk/data_request/cif.

References

[1] M. Mohan, M.P. Gupta, L. Chandra, N.K. Jha, Synthesis, characterization and antitumour properties of some metal(II) complexes of 2-pyridinecarboxaldehyde 2′-pyridylhydrazone and related compounds, Inorg. Chim. Acta 151 (1988) 61–68.

[2] D.R. Richardson, P. Ponka, Development of iron chelators to treat iron overload disease and their use as experimental tools to probe intracellular iron metabolism, Am. J. Hematol. 58 (1998) 299–305.

[3] D.S. Kalinowski, P.C. Sharpe, P.V. Bernhardt, D.R. Richardson, Structure-activity relationships of novel iron chelators for the treatment of iron overload disease: the methyl pyrazinylketone isonicotinoyl hydrazone series, J. Med. Chem. 51 (2008) 331–344.

[4] P.V. Bernhardt, P. Chin, P.C. Sharpe, J-Y.C. Wang, D.R. Richardson, Novel diaroyl-hydrazine ligands as iron chelators: coordination chemistry and biological activity, J. Biol. Inorg. Chem. 10 (2005) 761–777.

[5] G. Tamasi, L. Chiasserini, L. Savini, A. Sega, R. Cini, Structural study of ribonucleotide reductase inhibitor hydrazones. Synthesis and X-ray diffraction analysis of a copper(II)-benzoylpyridine-2-quinolinyl hydrazone complex, J. Inorg. Biochem. 99 (2005) 1347–1359.

[6] R.A. de Souza, A. Stevanato, O. Treu-Filho, A.V.G. Netto, A.E. Mauro, E.E. Castellano, I.Z. Carlos, F.R. Pavan, C.Q.F. Leite, Antimycobacterial and antitumor activities of palladium(II) complexes containing isonicotinamide (isn): X-ray structure of *trans*-$[Pd(N_3)_2(isn)_2]$, Eur. J. Med. Chem. 45 (2010) 4863–4868.

[7] B. Shaabani, A. A. Khandar, M. Dusek, M. Pojarova, M.A. Maestro, R. Mukherjee, F. Mahmoudi, Synthesis, crystal structures, antimicrobial activities, and DFT calculations of two new azido nickel(II) complexes, J. Coord. Chem. 67 (2014) 2096–2109.

[8] M. Milenković, A. Pevec, I. Turel, M. Milenković, B. Čobeljić, D. Sladić, N. Krstić, K. Anđelković, Synthesis, crystal structures, and antimicrobial activity of square-planar chloride and isocyanate Ni(II) complexes with the condensation product of 2-(diphenylphosphino)benzaldehyde and Girard's T reagent, J. Coord. Chem. 68 (2015) 2858–2870.

[9] S.K. Dey, N. Mondal, M. Salah El Fallah, R. Vicente, A. Escuer, X. Solans, M. Font-Bardía, T. Matsushita, V. Gramlich, S. Mitra, Crystal structure and magnetic interactions in nickel(II) dibridged complexes formed by two azide groups or by both phenolate oxygen-azide, -thiocyanate, -carboxylate, or -cyanate groups, Inorg. Chem. 43 (2004) 2427–2434.

[10] S.S. Massoud, F.R. Louka, Y.K. Obaid, R. Vicente, J. Ribas, R. C. Fischer, F.A. Mautner, Metal ions directing the geometry and nuclearity of azido-metal(II) complexes derived from bis(2-(3,5-dimethyl-1*H*-pyrazol-1-yl)ethyl)amine, Dalton Trans. 42 (2013) 3968–3978.

[11] (a) M. Nandy, S. Shit, E. Garribba, C.J. Gómez-García, S. Mitra, Double azido/cyanato bridged copper(II) dimers incorporating tridentate nitrogen donors Schiff base: Structure, EPR and magnetic studies, Polyhedron 102 (2015) 137–146; (b) F. A. Mautner, M. Scherzer, C. Berger, R. C. Fischer, R. Vicente, S. S. Massoud, Synthesis and characterization of five new thiocyanato- and cyanato-metal(II) complexes with 4-azidopyridine as co-ligand, Polyhedron 85 (2015) 20–26.

[12] A. H. Norbury, A. I. P. Sinha, The co-ordination of ambidentate ligands, Q. Rev. Chem. Soc. 24 (1970) 69–94.

[13] O. Kahn, Y. Pei, Y. Journaux, In Inorganic Materials, second ed., Q. W. Bruce, D. O'Hare, Eds.; John Wiley & Sons, Chichester, U.K., 1997.

[14] J. Ribas, A. Escuer, M. Monfort, R. Vicente, R. Cortés, L. Lezama, T. Rojo, Polynuclear Ni^{II} and Mn^{II} azido bridging complexes. Structural trends and magnetic behavior, Coord. Chem. Rev. 193–195 (1999) 1027–1068.

[15] M.Č. Romanović, M.R. Milenković, A. Pevec, I. Turel, V. Spasojević, S. Grubišić, D. Radanović, K. Anđelković, Božidar Čobeljić, Crystal structures, magnetic properties and DFT study of cobalt(II) azido complexes with the condensation product of 2-quinoline-carboxaldehyde and Girard's T reagent, Polyhedron 139 (2018) 142–147.

[16] M.Č. Romanović, B.R. Čobeljić, A. Pevec, I. Turel, V. Spasojević, A. A. Tsaturyan, I. N. Shcherbakov, K. K. Anđelković, M. Milenković, D. Radanović, M.R. Milenković, Synthesis, crystal structure, magnetic properties and DFT study of dinuclear Ni(II) complex with the condensation product of 2-quinolinecarboxaldehyde and Girard's T reagent, , Polyhedron 128 (2017) 30–37.

[17] M. Č. Romanović, B. Čobeljić, A. Pevec, I. Turel, K. Anđelković, M. Milenković, D. Radanović, S. Belošević, M. R. Milenković, Synthesis, crystal structures and antimicrobial activity of azido and isocyanato Zn(II) complexes with the condensation product of 2-quinolinecarboxaldehyde and Girard's T reagent, J. Coord. Chem. 70 (2017) 2425–2435.

[18] M. Č. Romanović, B. Čobeljić, A. Pevec, I. Turel, S. Grubišić, D. Radanović, K. Anđelković, M. Milenković, M. R. Milenković, Synthesis, characterization, DFT calculations and antimicrobial activity of Cd(II) complexes with the condensation product of 2-quinolinecarboxaldehyde and Girard's T reagent, J. Coord. Chem. 70 (2017) 3702–3714.

[19] Z. Otwinowsky, W. Minor, Macromolecular Crystallography, Methods Enzymol. 276 (1997) 307–326.

[20] Oxford Diffraction, CrysAlis PRO, Oxford Diffraction Ltd., Yarnton, England, 2009.

[21] A. Altomare, G. Cascarano, C. Giacovazzo, A. Guagliardi, Completion and refinement of crystal structures with *SIR*92, J. Appl. Crystallogr. 26 (1993) 343–350.

[22] G.M. Sheldrick, Crystal structure refinement with *SHELXL*, Acta. Crystallogr. C71 (2015) 3–8.

[23] P. Müller, Practical suggestions for better crystal structures, Crystallogr. Rev. 15 (2009) 57–83.

[24] L. J. Farrugia, WinGX and ORTEP for Windows: an update, J. Appl. Crystallogr. 45 (2012) 849–854.

[25] M. J. Frisch, G. W. Trucks, H. B. Schlegel, G. E. Scuseria, M. A. Robb, J. R. Cheeseman, G. Scalmani, V. Barone, B. Mennucci, G. A. Petersson, H. Nakatsuji, M. Caricato, X. Li, H. P. Hratchian, A. F. Izmaylov, J. Bloino, G. Zheng, J. L. Sonnenberg, M. Hada, M. Ehara, K. Toyota, R. Fukuda, J. Hasegawa, M. Ishida, T. Nakajima, Y. Honda, O. Kitao, H. Nakai, T. Vreven, J. A. Montgomery Jr., J. E. Peralta, F. Ogliaro, M. Bearpark, J. J. Heyd, E. Brothers, K. N. Kudin, V. N. Staroverov, R. Kobayashi, J. Normand, K. Raghavachari, A. Rendell, J. C. Burant, S. S. Iyengar, J. Tomasi, M. Cossi, N. Rega, J. M. Millam, M. Klene, J. E. Knox, J. B. Cross, V. Bakken, C. Adamo, J. Jaramillo, R. Gomperts, R. E. Stratmann, O. Yazyev, A. J. Austin, R. Cammi, C. Pomelli, J. W. Ochterski, R. L. Martin, K. Morokuma, V. G. Zakrzewski, G. A. Voth, P. Salvador, J. J. Dannenberg, S. Dapprich, A. D. Daniels, Ö. Farkas, J. B. Foresman, J. V. Ortiz, J. Cioslowski and D. J. Fox, *Gaussian 09 (Revision D.01)*, Gaussian, Inc., Wallingford CT, 2009

[26] A. D. Becke, Density□functional thermochemistry. III. The role of exact exchange, J. Chem. Phys. 98 (1993) 5648–5652.

[27] C. Lee, W. Yang, R. G. Parr, Development of the Colle-Salvetti correlation-energy formula into a functional of the electron density, Phys. Rev. B 37 (1988) 785–789.

[28] W. R. Wadt, P. J. Hay, *Ab initio* effective core potentials for molecular calculations. Potentials for main group elements Na to Bi, J. Chem. Phys. 82 (1985) 284–298; P. J. Hay, W. R. Wadt, *Ab initio* effective core potentials for molecular calculations. Potentials for K to Au including the outermost core orbitals, ibid. 82 (1985) 299–310; P. J. Hay, W. R. Wadt, *Ab initio* effective core potentials for molecular calculations. Potentials for the transition metal atoms Sc to Hg, ibid. 82 (1985) 270–283.

[29] W.J. Hehre, R. Ditchfield, J. A. Pople, Self-consistent molecular orbital methods. XII. Further extensions of Gaussian-Type basis sets for use in molecular orbital studies of organic molecules, J. Chem. Phys. 56 (1972) 2257–2261; P. C. Hariharan, J. A. Pople, The influence of polarization functions on molecular orbital hydrogenation energies, Theor. Chim. Acta 28 (1973) 213–222.

[30] PARADOX IV cluster at the Scientific Computing Laboratory of the Institute of Physics Belgrade, supported in part by the Serbian Ministry of Education and Science under project No. ON171017.

[31] A. W. Addison, T. N. Rao, J. Reedijk, J. Van Rijn, G. C. Verschoor, Synthesis, structure, and spectroscopic properties of copper(II) compounds containing nitrogen–sulphur donor ligands; the crystal and molecular structure of aqua[1,7-bis(*N*-methylbenzimidazol-2′-yl)-2,6-dithiaheptane]copper(II) perchlorate , J. Chem. Soc., Dalton Trans. (1984) 1349–1356.

[32] J. L. Pascual-Ahuir, E. Silla, J. Tomasi, R. Bonaccorsi, Electrostatic interaction of a solute with a continuum. Improved description of the cavity and of the surface cavity bound charge distribution, J. Comput. Chem. 8 (1987) 778–787.

[33] V. Barone, M. Cossi, J. Tomasi, A new definition of cavities for the computation of solvation free energies by the polarizable continuum model, J. Chem. Phys. 107 (1997) 3210–3221.

[34] R. A. Pierotti, A scaled particle theory of aqueous and nonaqueous solutions, Chem. Rev. 76 (1976) 717–726.

[35] F. Floris, J. Tomasi, Evaluation of the dispersion contribution to the solvation energy. A simple computational model in the continuum approximation, J. Comput. Chem. 10 (1989) 616–627.

[36] J. Tomasi, B. Mennucci, R. Cammi, Quantum mechanical continuum solvation models, Chem. Rev. 105 (2005) 2999–3094.

Table captions

Table 1. Crystal data and structure refinement details for **1** and **2**.

Table 2. Selected bond lengths (Å) and angles (°) for **1** and **2**.

Table 3. Intermolecular C–H···π(quinoline ring) interaction parameters for complex **1**.

Table 4. Intermolecular π···π interaction parameters for complexes **1** and **2**.

Table 5. DFT calculated binding energies.

Table 1. Crystal data and structure refinement details for **1** and **2**.

	1	**2**
formula	$C_{15}H_{18}Cl_{0.35}N_{8.94}OZn$	$C_{16.64}H_{18}CdCl_{0.36}N_{5.64}O_{2.64}$
Fw (g mol^{-1})	417.44	464.38
crystal size (mm)	0.20 × 0.10 × 0.05	0.20 × 0.18 × 0.15
crystal color	yellow	yellow
crystal system	triclinic	triclinic
space group	*P* –1	*P* –1
a (Å)	8.5326(2)	7.8143(4)
b (Å)	10.1887(4)	10.3420(4)
c (Å)	11.1952(4)	12.4059(5)
α (°)	113.052(2)	76.279(4)
β (°)	90.948(2)	80.148(4)
γ (°)	97.611(2)	73.700(4)
V (Å^3)	885.16(5)	928.94(7)
Z	2	2
calcd density (g cm^{-3})	1.566	1.660
F(000)	429	465
no. of collected reflns	6990	8482
no. of independent reflns	3996	4261
R_{int}	0.0156	0.0302
no. of reflns observed	3606	3634
no. parameters	260	254
$R[I > 2\sigma(I)]$[a]	0.0316	0.0400
wR_2 (all data)[b]	0.0848	0.1052
Goof , *S*[c]	1.140	1.070
maximum/minimum residual electron density (e Å^{-3})	+0.27/–0.32	+0.94/–0.79

[a] $R = \sum||F_o| - |F_c||/\sum|F_o|$. [b] $wR_2 = \{\sum[w(F_o^2 - F_c^2)^2]/\sum[w(F_o^2)^2]\}^{1/2}$.
[c] $S = \{\sum[(F_o^2 - F_c^2)^2]/(n/p)\}^{1/2}$ where *n* is the number of reflections and *p* is the total number of parameters refined.

Table 2. Selected bond lengths (Å) and angles (°) for **1** and **2**.

1		**2**	
Zn1-N8	1.980(9)	Cd1-N6	2.170(12)
Zn1-N5	1.990(2)	Cd1-N5	2.179(4)
Zn1-N2	2.057(2)	Cd1-N2	2.263(3)
Zn1-N1	2.240(2)	Cd1-N1	2.416(3)
Zn1-O1	2.222(2)	Cd1-O1	2.370(3)
Zn1-Cl1	2.289(5)	Cd1-Cl1	2.480(4)
N2-N3	1.387(2)	N2-N3	1.383(4)
N2-C10	1.276(3)	N2-C10	1.279(5)
N3-C11	1.330(3)	N3-C11	1.334(5)
O1-C11	1.255(3)	O1-C11	1.255(4)
N5-N6	1.185(3)	N5-C16	1.078(5)
N6-N7	1.152(3)	N6-C17	1.30(2)
N8-N9	1.155(11)	C16-O2	1.212(6)
N9-N10	1.159(8)	C17-O3	1.371(11)
N5-Zn1-N8	112.5(3)	N6-Cd1-N5	106.7(4)
N5-Zn1-N2	128.68(8)	N5-Cd1-N2	127.77(13)
N8-Zn1-N2	118.3(3)	N6-Cd1-N2	124.8(4)
N5-Zn1-N1	107.27(7)	N5-Cd1-N1	101.47(12)
N8-Zn1-N1	95.3(3)	N6-Cd1-N1	110.9(4)
N2-Zn1-N1	75.44(6)	N2-Cd1-N1	70.09(10)
N5-Zn1-O1	93.23(7)	N5-Cd1-O1	102.26(12)
N8-Zn1-O1	98.8(4)	N6-Cd1-O1	94.3(4)
N2-Zn1-O1	72.97(6)	N2-Cd1-O1	68.34(10)
N1-Zn1-O1	148.40(6)	N1-Cd1-O1	138.39(9)
N2-Zn1-Cl1	125.8(2)	N2-Cd1-Cl1	127.8(2)
N5-Zn1-Cl1	105.0(2)	N5-Cd1-Cl1	104.5(2)
O1-Zn1-Cl1	99.9(2)	O1-Cd1-Cl1	103.8(2)
N1-Zn1-Cl1	97.7(2)	N1-Cd1-Cl1	102.64(14)
N6-N5-Zn1	118.8(2)	C16-N5-Cd1	155.3(4)
N9-N8-Zn1	120.8(9)	C17-N6-Cd1	119.5(8)
N7-N6-N5	176.7(2)	N5-C16-O2	177.4(5)
N8-N9-N10	176.2(8)	N6-C17-O3	173.9(10)

Table 3. Intermolecular C–H···π(quinoline ring) interaction parameters for complex **1**.

C–H	Cg(J)	H···Cg (Å)	H···(quinoline J)[a] (Å)	C–H···Cg (°)	γ[b] (°)	Sym. code on (J)
C13-H13C	Cg(2)	2.98	-2.82	131	18.84	x, y, 1+z

[a] Perpendicular distance of H to ring plane (J) (Ang.).
[b] γ = Angle between H···Cg line and perpendicular H···(ring plane) line (Deg.).

Table 4. Intermolecular π···π interaction parameters for complexes **1** and **2**.

Cg(I)[a]	Cg(J)[a]	Cg(I) –Cg(J)[b] (Å)	α[c] (°)	β[d] (°)	γ[e] (°)	Slippage[f] (Å)	Sym. code on (J)
complex **1**							
Cg(1)	Cg(1)	3.6481(12)	0.0	18.2	18.2	1.139	2-x,-y,2-z
Cg(1)	Cg(2)	4.2043(13)	1.34(10)	34.6	35.1		2-x,-y,2-z
complex **2**							
Cg(1')	Cg(1')	3.544(2)	0.0	19.6	19.6	1.186	-x,1-y,1-z
Cg(1')	Cg(2')	4.903(2)	0.7(2)	46.8	47.4		-x,1-y,1-z

[a] Labels of aromatic rings: complex **1** (1) = N(1),C(1)–C(4),C(9); (2) = C(4)–C(9);
complex **2** (1') = N(1),C(1)–C(4),C(9); (2') = C(4)–C(9).
[b] Cg(I) –Cg(J) = Distance between ring centroids (Ang.).
[c] α = Dihedral angle between planes (I) and (J) (Deg.).
[d] β = Angle between Cg(I)–Cg(J) vector and normal to plane (I) (Deg.).
[e] γ = Angle between Cg(I) –Cg(J) vector and normal to plane (J) (Deg.).
[f] Slippage = Distance between Cg(I) and perpendicular projection of Cg(J) on ring I (Ang.).

Table 5. DFT calculated binding energies.

	Intrinsic binding energy (kcal/mol)	Solvatation energy (kcal/mol)	Real binding energy (kcal/mol)
[Cd**L**$(NCO)_2$]	-698	-224 (methanol)/-222(water)	-474(methanol)/-476 (water)
[Cd**L**(NCO)Cl]	-696	-224 (methanol)/-222(water)	-472(methanol)/-474 (water)
[Zn**L**$(N_3)_2$]	-745	-229 (methanol)	-516 (methanol)
[Zn**L**(N_3)Cl]	-751	-229 (methanol)	- 522(methanol)

Scheme captions

Scheme 1. Coordination modes of azido ligand.

Scheme 2. Structure of (*E*)-*N*,*N*,*N*-trimethyl-2-oxo-2-(2-(quinolin-2-ylmethylene)hydrazinyl)ethan-1-aminium chloride (**HL**Cl).

Figure captions

Figure 1. ORTEP diagram of **1** showing separated representations of (a) [Zn**L**$(N_3)_2$] and (b) [Zn**L**(N_3)Cl] derived from the X-ray crystal structure of the mixed chloride-azide [Zn**L**$(N_3)_{1.65}Cl_{0.35}$]. Thermal ellipsoids are drawn at the 30% probability level.

Figure 2. ORTEP diagram of **2** showing separated representations of (a) [Cd**L**$(NCO)_2$] and (b) [Cd**L**(NCO)Cl] derived from the X-ray crystal structure of the mixed chloride-cyanate [Cd**L**$(NCO)_{1.64}Cl_{0.36}$]. Thermal ellipsoids are drawn at the 30% probability level.

Figure 3. Crystallographic autostereogram of **1**. 1D chains generated by intermolecular C-H···π interactions extend parallel with [001]. Dashed lines indicate C-H···π and π···π interactions. Thermal ellipsoids are drawn at the 30% probability level.

Figure 4. Packing diagram of **2** showing dimers formed *via* intermolecular π···π interactions around the center of symmetr at 0 ½ ½ (π···π interactions are indicated by dashed lines). Thermal ellipsoids are drawn at the 30% probability level.

Figure 5. DFT optimized geometries of a) [Cd**L**$(NCO)_2$]; b) [Cd**L**(NCO)Cl]; c) [Zn**L**$(N_3)_2$] and d) [Zn**L**(N_3)Cl].

Figure 6. Molecular orbital plots and energy levels of the HOMO, the LUMO and HOMO-LUMO transitions of a) [Cd**L**$(NCO)_2$]; b) [Cd**L**(NCO)Cl]; c) [Zn**L**$(N_3)_2$] and d) [Zn**L**(N_3)Cl].

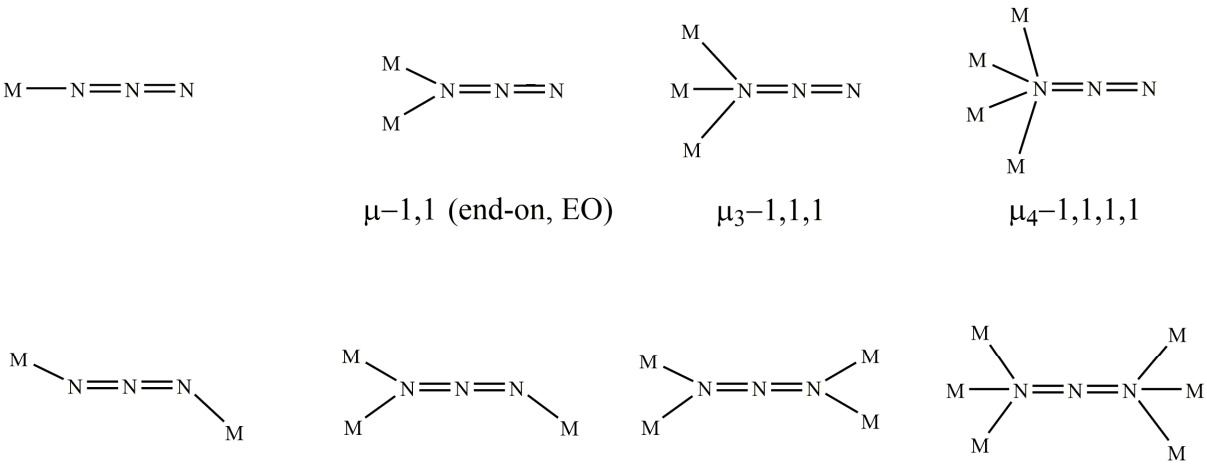

Scheme 1. Coordination modes of azido ligand.

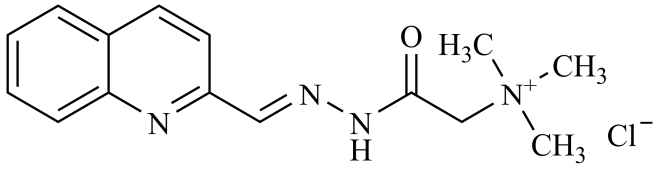

Scheme 2. Structure of (*E*)-*N*,*N*,*N*-trimethyl-2-oxo-2-(2-(quinolin-2-ylmethylene)hydrazinyl)ethan-1-aminium chloride (**HL**Cl).

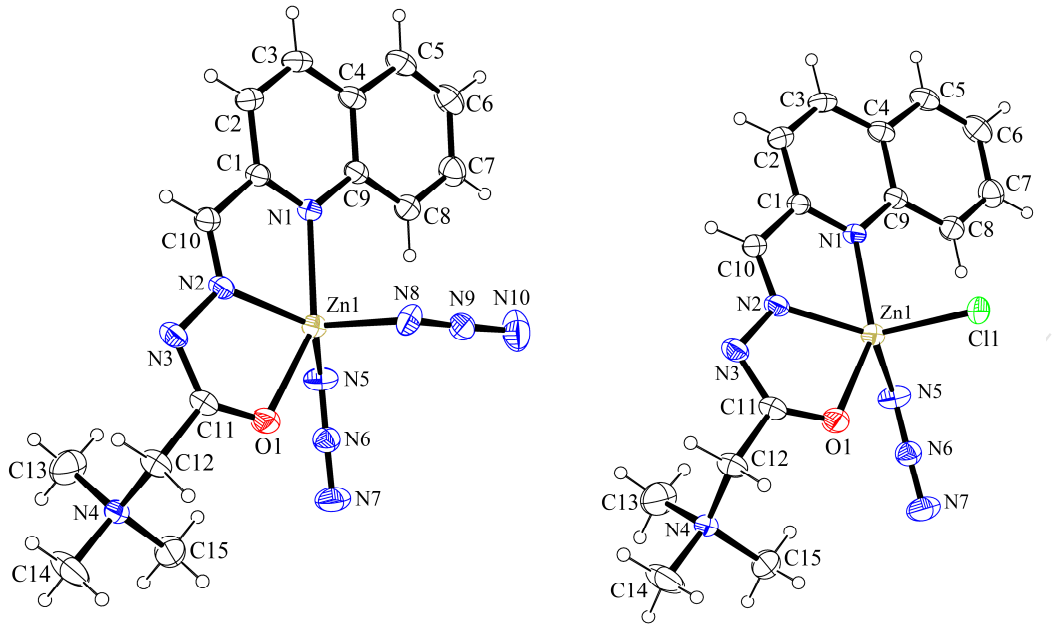

(a) (b)

Figure 1. ORTEP diagram of **1** showing separated representations of (a) [Zn**L**$(N_3)_2$] and (b) [Zn**L**(N_3)Cl] derived from the X-ray crystal structure of the mixed chloride-azide [Zn**L**$(N_3)_{1.65}Cl_{0.35}$]. Thermal ellipsoids are drawn at the 30% probability level.

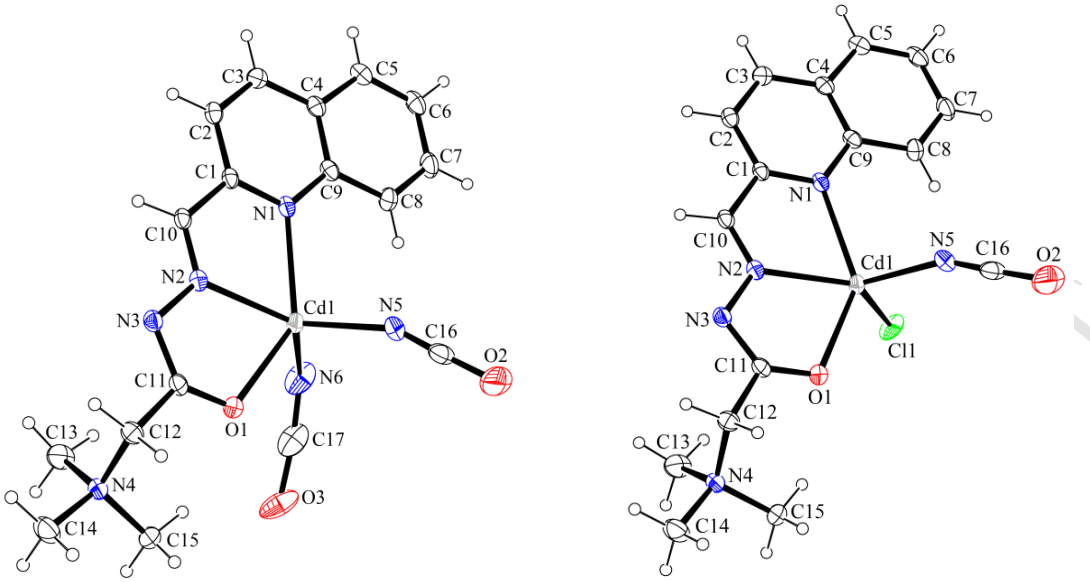

(a) (b)

Figure 2. ORTEP diagram of **2** showing separated representations of (a) [Cd**L**$(NCO)_2$] and (b) [Cd**L**(NCO)Cl] derived from the X-ray crystal structure of the mixed chloride-cyanate [Cd**L**$(NCO)_{1.64}Cl_{0.36}$]. Thermal ellipsoids are drawn at the 30% probability level.

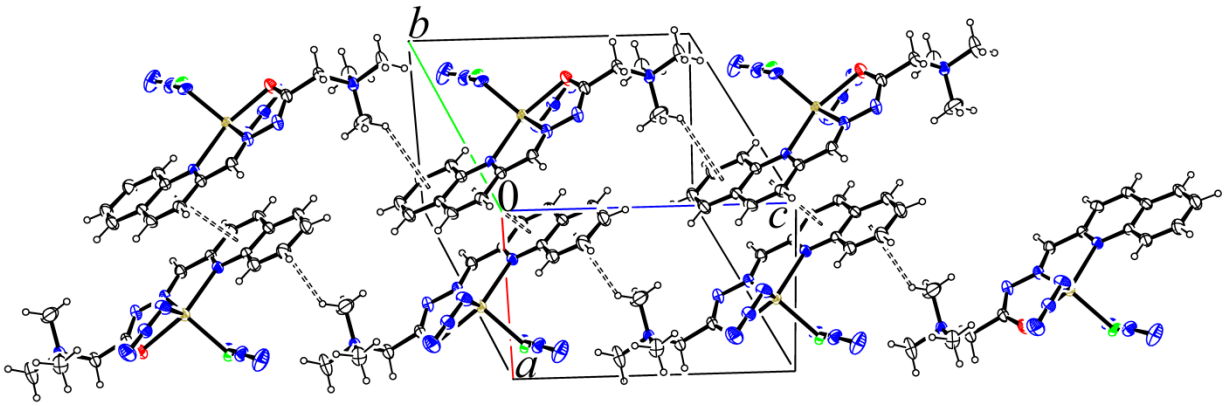

Figure 3. Crystallographic autostereogram of **1**. 1D chains generated by intermolecular C-H···π interactions extend parallel with [001]. Dashed lines indicate C-H···π and π···π interactions. Thermal ellipsoids are drawn at the 30% probability level.

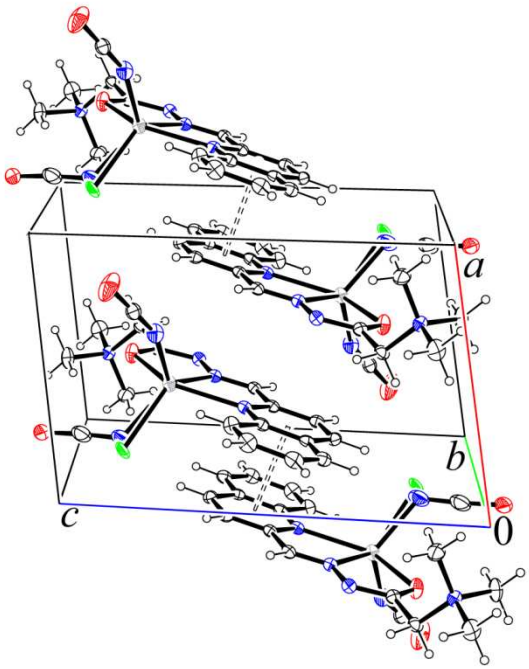

Figure 4. Packing diagram of **2** showing dimers formed *via* intermolecular π···π interactions around the center of symmetr at 0 ½ ½ (π···π interactions are indicated by dashed lines). Thermal ellipsoids are drawn at the 30% probability level.

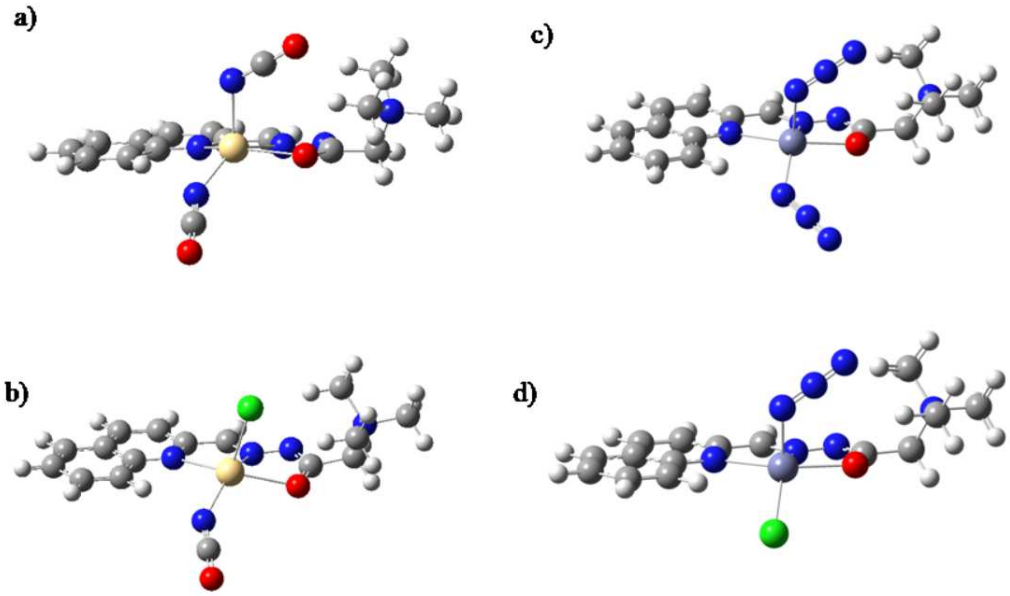

Figure 5. DFT optimized geometries of a) [Cd**L**$(NCO)_2$]; b) [Cd**L**(NCO)Cl]; c) [Zn**L**$(N_3)_2$] and d) [Zn**L**(N_3)Cl].

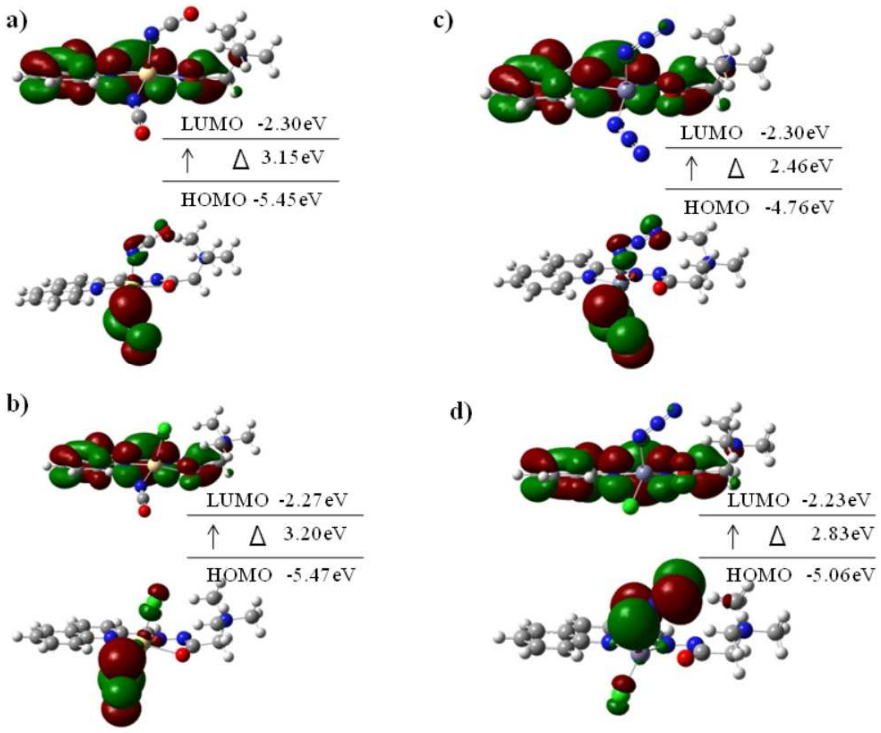

Figure 6. Molecular orbital plots and energy levels of the HOMO, the LUMO and HOMO-LUMO transitions of a) [Cd**L**$(NCO)_2$]; b) [Cd**L**(NCO)Cl]; c) [Zn**L**$(N_3)_2$] and d) [Zn**L**(N_3)Cl].

Highlights

- Structures of [Zn**L**$(N_3)_{1.65}Cl_{0.35}$] and [Cd**L**$(NCO)_{1.64}Cl_{0.36}$] were found by XRD.
- Zn(II) and Cd(II) ions adopt distorted square based pyramidal geometry.
- DFT method was applied to calculate metal-binding energies.